Characteristics of Sunward Flowing Proton and Alpha Particle Fluxes of Moderate Intensity

F. E. MARSHALL[1] AND E. C. STONE

California Institute of Technology, Pasadena, California 91125

The diffusive streaming of 1.3- to 2.3-MeV per nucleon protons has been found to be predominantly toward the sun during periods between prompt solar particle events. This sunward streaming occurs for essentially all proton intensities from <0.012 to 1.2 $(cm^2\ s\ sr\ MeV)^{-1}$ and for all solar wind velocities. The average radial component (16% ± 3%) of the diffusive anisotropy of 1.4- to 2.4-MeV per nucleon alpha particles is very similar to that observed for protons (14% ± 1%), a finding suggesting a common origin. These periods are characterized by a limited variance in the proton intensities ($10^{-1.2\pm1.1}$ $cm^{-2}\ s^{-1}\ sr^{-1}\ MeV^{-1}$), in the proton spectra ($E^{-3.0\pm0.8}$), and in the α/p ratio (3% ± 2%). The sunward diffusion of protons and alpha particles indicates that a positive radial gradient is characteristic of these modestly enhanced fluxes. A steady state propagation model which includes adiabatic energy loss and a source of particles beyond 1 AU produces the average radial anisotropy and its dependence on the solar wind velocity for $\kappa_{rr} \sim 4 \times 10^{20}$ $cm^2\ s^{-1}$. The direction of the diffusive anisotropy is strongly dependent on the magnetic field direction, a situation indicating $\kappa_\perp < \kappa_\parallel$. However, the two directions are not identical, a condition indicating nonnegligible flow perpendicular to the average field direction when averaged over a 6-hour interval.

INTRODUCTION

The flux of 1.3- to 2.3-MeV protons at 1 AU exhibits enormous variations. The periods of largest flux are due to prompt solar particle events, which have been studied by many investigators (see the review by *McCracken and Rao* [1970]); these periods will not be discussed herein. However, even between prompt events the flux varies over several orders of magnitude. Individual increases, or events, have been studied by *Bryant et al.* [1965], *Fan et al.* [1965, 1968], *Anderson* [1969], *McDonald and Desai* [1971], *Krimigis et al.* [1971], and *Roelof and Krimigis* [1973]. Unlike prompt solar events these increases have slower rise times, rather symmetric time profiles, and no velocity dispersion. These studies led to a model for these increases in which the particles are accelerated at the sun and then continuously injected into the interplanetary medium. Since these increases tend to recur with the solar rotation period, they have been referred to as recurrent or corotating events. A study of more extended periods by *Kinsey* [1970] pictured the sun as a continuous but variable source of low-energy protons.

At energies lower than those included in the present work, *Krimigis et al.* [1971] reported anisotropies indicative of continuous streaming from the sun. Similar measurements have not been reported at higher energies.

On the other hand, measurements near 3 AU reported by *McDonald et al.* [1976] suggest that there is a source of MeV protons beyond 1 AU. Such a source might contribute significantly to the flux seen at 1 AU. In this case the particles would be diffusing back toward the sun. McDonald et al. found that the average intensity of recurrent events at 3 AU was about 10 times as large as recurrent events at 1 AU from September 1973 to March 1974. Interplanetary acceleration was suggested as the most likely source for the streams seen near 3 AU.

In a preliminary report, *Marshall and Stone* [1977] found protons to be diffusing predominantly toward the sun during periods between prompt events, a process indicating a predominantly positive radial gradient in the particle density. In the present paper we report details of those observations together with the dependence of the proton anisotropy on intensity, on alpha-to-proton ratio, on interplanetary magnetic field direction and fluctuations, and on solar wind velocity. The present paper also includes periods of high solar wind speed which were not included in the preliminary report. The average anisotropies for this slightly larger data set are only minimally different from those previously reported, with diffusive flow still predominantly toward the sun. We also find the average diffusive flow of 1.4- to 2.4-MeV per nucleon alpha particles to be nearly the same as that of 1.3- to 2.3-MeV protons.

DATA ANALYSIS

Jokipii and Parker [1970] have shown that in the anisotropic diffusion approximation the observed anisotropy is the sum of a convective anisotropy and a diffusive anisotropy:

$$\xi_{obs} = \xi_{con} + \xi_{dif} = \frac{3}{w}[C(\mathbf{V} - \mathbf{V}_E) - \kappa \cdot \nabla U/U] \qquad (1)$$

in which U is particle density, equal to $4\pi j/w$; $\mathbf{V}$ is solar wind velocity; $\mathbf{V}_E$ is velocity of the earth about the sun; κ is the diffusion tensor; w is particle velocity; C is the Compton-Getting factor, equal to $(2 + \alpha\gamma)/3$; $\alpha = (T + 2mc^2)/(T + mc^2)$; $\gamma = -\partial \ln j/\partial \ln T$; j is particle intensity; and T is particle kinetic energy. Thus to determine ξ_{dif}, which is related to the gradients in the particle density, ξ_{con} has been calculated and subtracted from the observed anisotropy.

Energetic particle data from the California Institute of Technology electron/isotope spectrometer (EIS) aboard Imp 7 have been used to measure ξ_{obs}. Details of the data analysis techniques are described by *Marshall* [1977] and are summarized here. Anisotropies are determined for nuclei which stop in D2, a 47-μm solid-state detector, and are pulse height analyzed (the instrument has been described by *Hurford et al.* [1974]). The omnidirectional intensity of all nuclei (primarily 1.2- to 2.4-MeV protons) stopping in D2 is measured by the PLO (low-energy proton) rate. There are two energy intervals of interest in the pulse height analyzed data corresponding to 1.3- to 2.3-MeV protons and 1.4- to 2.4-MeV per nucleon

[1] Present address: Goddard Space Flight Center, Greenbelt, Maryland 20771.

Paper number 8A0221.
0148-0227/78/078A-0221$01.00

alpha particles. Heavier nuclei which deposit the same total energy in D2 as the protons or alpha particles contribute $\lesssim 10^{-3}$ of the events in the intervals and thus negligibly affect the anisotropies. Similarly, alpha particles with 1.09–1.23 MeV per nucleon will deposit the same total energy in D2 as 1.3- to 2.3-MeV protons (D2 is behind a 2.4-mg/cm² aluminized mylar window). Since the number of alpha particles in this narrow energy interval will typically be only ~3% of the number of 1.3- to 2.3-MeV protons, the proton anisotropy will be negligibly affected.

Each analyzed event is labeled to indicate in which of eight sectors in the ecliptic plane it was observed; ξ_{obs} is determined by fitting the number of events observed in sector i with the function

$$A_0[1 + \xi \cos(\phi_0 - \phi_i)] \quad (2)$$

in which ϕ_i is the average direction of sector i. The anisotropy direction, which is the direction toward which the particles are flowing, is defined to be $\phi_0 + 180°$, and the anisotropy amplitude is 1.08ξ. The factor 1.08 corrects for the smoothing effect of the finite sector width and the finite angular response of the instrument. The solar ecliptic (SE) coordinate system, in which the x axis points toward the sun and the z axis points toward the north ecliptic pole, has been used.

The functional form of (2) is found to provide a reasonable fit to the data. A goodness-of-fit parameter is defined in the usual way:

$$\chi_\nu^2 = \left\{\sum[y_i - y(x_i)]/\sigma_i^2\right\}/\nu$$

in which y_i are the data points, σ_i their uncertainty, $y(x_i)$ the fitting function, and ν the number of degrees of freedom for the fit. The mean value of χ_ν^2 for the periods when the flux is greater than 0.04 (cm² s sr MeV)$^{-1}$ (data set 4*b*; see below) is 1.3, indicating that deviations of the observations from the functional fit are dominated by statistical uncertainties.

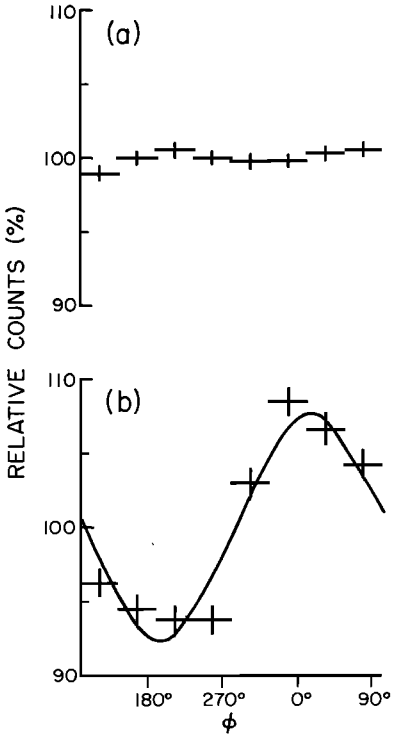

Fig. 1. (*a*) The relative number of ELO (low-energy electron) events by spacecraft viewing direction for 501 periods from day 273, 1972, to day 106, 1975, when the ELO rate is ≤0.0531/s. As was discussed in the text, these events are primarily instrumental background. The anisotropy amplitude observed is consistent with zero and is less than 0.5% at a 95% confidence level. (*b*) The relative number of D2 events for 195 of the periods in data set 4*b*.

The chi square test shows that (2) provides a good fit to the individual periods. The fit of (2) to an accumulation of 195 typical periods from data set 4*b* is shown in Figure 1*b*. It is seen that a first-order anisotropy provides a reasonable description of the data. The proton anisotropy of 8% shown in Figure 1*b* contrasts sharply with the lack of anisotropy (<0.5%) for events shown in Figure 1*a*. The counts of Figure 1*a* are independently known to be due to a nearly isotropic background. As was described by *Hurford et al.* [1974], these events are produced by gamma rays Compton-scattering in a 1-mm-thick solid-state detector. The gamma rays are generated from the interaction of high-energy (~1 GeV) cosmic rays in the spacecraft. This process is largely independent of the orientation of the spacecraft. Thus the small anisotropy measured for these events indicates that the 8% anisotropy for the protons corresponds to actual proton streaming.

As was shown in (1), ξ_{con} depends on $\mathbf{V}$, $\mathbf{V}_E$, γ, and w^{-1}. The spectral index γ is determined by fitting the energy spectrum observed by the EIS experiment, and w^{-1} is determined by averaging w^{-1} over the observed spectrum. The observed energy losses of 1.3- to 2.3-MeV protons are grouped into nine energy bins, and the events with these energy losses are accumulated. The counts are then corrected for stopping heavier nuclei by extrapolating the spectrum of heavier nuclei observed at higher energies. A correction is also made for particles which penetrate D2 but do not trigger another detector. A power law spectrum is then fit to the corrected counts. The mean value of χ_ν^2 for these power law fits when the flux is greater than 0.04 (cm² s sr MeV)$^{-1}$ (data set 4*b*; see below) is 1.3, indicating that a power law spectrum provides a reasonable fit to the data. There was a 17-day interval during which the operational mode of the instrument resulted in a small systematic uncertainty in the spectra. However, the average properties of this period were not statistically different from those of the complete period, and therefore these observations were included in the following analysis.

Hourly averages of $\mathbf{V}$ have been obtained from the Massachusetts Institute of Technology plasma experiment on Imp 7 (J. D. Sullivan and H. S. Bridge, private communication, 1976) and are assumed to be radial. These hourly averages have been combined to form the 6-hour averages used in this study. The relative rms variation of the velocity is less than 5% for more than 90% of the 6-hour periods, indicating that V is relatively constant during the 6-hour periods. Unlike the preliminary report of this work [*Marshall and Stone,* 1977] this paper includes all solar wind speeds. $\mathbf{V}_E$ is assumed constant with a value of 30 km/s in the $-y_{SE}$ direction.

Since ξ_{dif} is determined by subtracting ξ_{con} from ξ_{obs}, errors in γ or V which cause an error in ξ_{con} will result in an error in ξ_{dif}. One such error could be introduced by the averaging technique for V if the intensity is correlated with V on a 1-hour time scale. The amount of correlation (if any) is unknown, but the error must be less than the variation in V during the 6-hour period. Even this upper limit results in an error in ξ_{dif} of $\lesssim 1\%$. Systematic errors in the measurement of V would also introduce errors in ξ_{con}, but even an error of 20 km/s results in an error of only ~1% in ξ_{dif}.

It has been assumed that the energy spectra are power laws in kinetic energy, and this functional form does provide a good fit to the observations. Other functional forms are possible.

TABLE 1. Data Set Characteristics for the Period From Day 273, 1972, to Day 2, 1974

Data Set	Flux Interval, $(cm^2\ s\ sr\ MeV)^{-1}$	Characteristics
1	all	all available energetic particle data
2	all	Imp 7 sunward of earth
3	all	concurrent **B** and V available
4*a*	0–1.2	prompt events excluded
4*b*	0.04–1.2	
4*c*	0.12–1.2	

Note that a given data set is a subset of the data sets above it in the table.

Using the incorrect functional form produces small errors in ξ_{con}. For example, if the spectra were actually an exponential in rigidity, using a power law representation would result in a systematic underestimate of only 0.3% in ξ_{dif}. Even these upper limits to the uncertainty in ξ_{dif} are a small fraction of the average ξ_{dif} of ~15% and so cannot significantly affect the results of this study.

Magnetic field information, which will be correlated with the proton anisotropy, has been obtained from the National Space Science Data Center. The primary sources of these data are the Imperial College magnetometers aboard the earth-orbiting Heos 1 and 2 satellites. The field direction used for a 6-hour period is determined from the available 1-hour averages by computing

$$\mathbf{B}_{6\text{-hour}}^{*} = \langle \mathbf{B}_{1\text{-hour}} / |B_{1\text{-hour}}| \rangle$$

The direction defined by the projection of $B_{6\text{-hour}}^{*}$ onto the ecliptic plane is used as the 6-hour average field direction. The field direction can differ significantly from the average direction during the 6-hour period. The standard deviation of the 1-hour values about the 6-hour average is 36°.

Data Selection

Various selection criteria have been used for the different investigations reported in this paper. The rationale for the criteria will be discussed in this section. Table 1 lists the data sets and the selection criteria.

Data set 1 is the largest set, containing all of the energetic particle data available from Imp 7 through day 2, 1974. This set contains 94% of the 6-hour periods between day 273, 1972, and day 2, 1974.

Data set 2 is chosen to avoid magnetospheric influence and consists of those periods of data set 1 when Imp 7 is sunward of the earth. There are 851 6-hour periods in data set 2. The dependence of ξ_{obs} on the position of Imp 7 has been examined to determine any remaining magnetospheric influence. We previously found no significant dependence of $|\xi_{obs}|$ on the position of Imp 7 when the satellite is sunward of the earth [*Marshall and Stone,* 1977]. Figure 2 shows ξ_{obs} for those periods in an extended data set for which the flux is between 0.12 and 1.2 $(cm^2\ s\ sr\ MeV)^{-1}$ and the spacecraft is sunward of the earth. Figures 2*a* and 2*b* consist of data for the dawn and the dusk sunward quadrant, respectively. The mean ξ_{obs} for the quadrants differ in their x and y components by 1.3% and 1.7%, respectively. The differences are not significant at the 80% confidence level, a finding indicating no significant magnetospheric effect. Thus we find no evidence for a magnetospheric effect either in $|\xi_{obs}|$ or in $\langle \xi_{obs} \rangle$.

Data set 3 consists of those periods of data set 2 for which concurrent magnetic field and solar wind speed data are available.

Data set 4 is a subset of data set 3 in which periods in data set 3 dominated by prompt solar particle events have been rejected by setting a maximum flux of 1.2 $(cm^2\ s\ sr\ MeV)^{-1}$. In addition, 25 individual prompt events were identified by characteristically rapid onsets on the following days, where on those days in italics there was also observed rapid onset of electrons ($E \gtrsim 200$ keV) observed within 1 day: in 1972, days *282*, 291, *303*, *329*, *333*, 348, and *351*; in 1973, days *46*, *71*, 78, 89, *102*, *114*, *119*, 154, *171*, *180*, *210*, *250*, *261*, 270, 277, 292, *307*, and 310. The day before the onset (to avoid small precursors) and the next 3 days were not used. Anisotropy data were not part of the rejection criteria. Those periods in data set 3 which were not rejected to avoid prompt events comprise data set 4 (381 periods).

For many of the investigations of this study, a lower flux limit is an additional criterion. For data sets 4*a*, 4*b*, and 4*c* the lower limits are 0, 0.04, and 0.12 $(cm^2\ s\ sr\ MeV)^{-1}$, respectively. All of the data sets are summarized in Table 1. Most investigations use either data set 4*b* (which includes 229 peri-

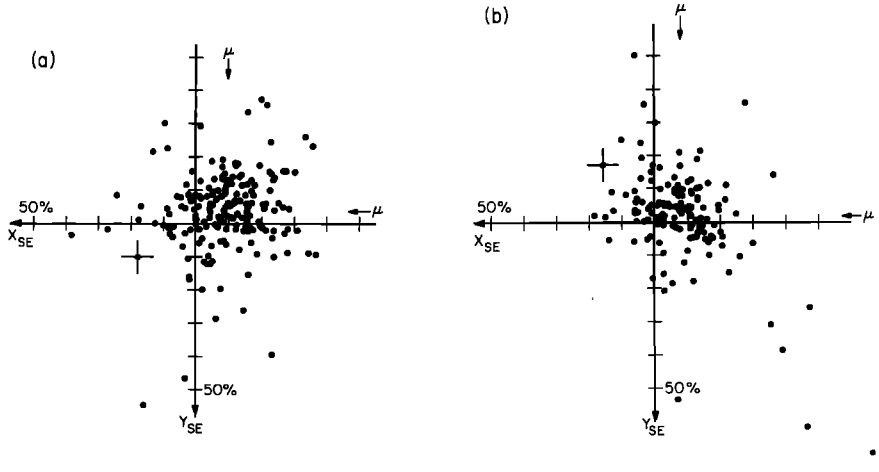

Fig. 2. (*a*) The observed anisotropy ξ_{obs} when Imp 7 is sunward and on the dawnside of the earth. The data are from day 273, 1972, to day 18, 1975. Periods dominated by prompt solar particle events are not used. The proton flux for each period is between 0.12 and 1.2 $(cm^2\ s\ sr\ MeV)^{-1}$. The mean x and y components of ξ_{obs}, which are indicated by arrows, are $-9.1\% \pm 0.7\%$ and $-3.9\% \pm 0.7\%$. (*b*) The observed anisotropy ξ_{obs} when Imp 7 is sunward and on the duskside of the earth. The mean x and y components are $-7.8\% \pm 1.1\%$ and $-2.2\% \pm 1.2\%$.

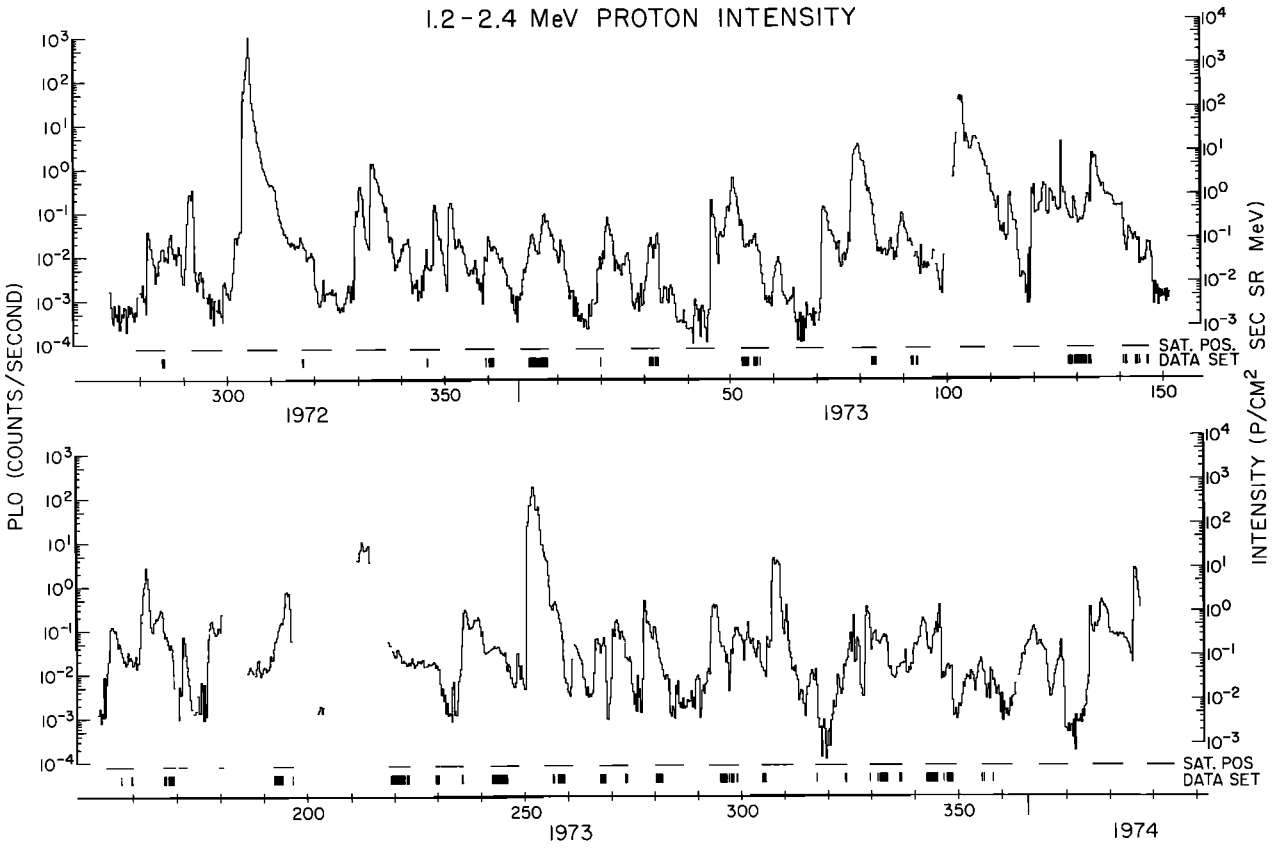

Fig. 3. The 6-hour averages of the PLO rate for data set 1. The PLO rate monitors nucleons (primarily 1.2- to 2.4-MeV protons) stopping in D2. The corresponding proton intensities are shown by the right-hand scale. Periods when Imp 7 is sunward of the earth are indicated. Periods in data set 4*b* are also shown.

ods) or 4*c* (122 periods), which are periods of moderately enhanced fluxes between prompt events.

The intensity of 1.2- to 2.4-MeV protons is plotted as a function of time in Figure 3 for the time span day 273, 1972, to day 28, 1974. Periods in data set 4*b* are also indicated. Note that the periods tend to cluster owing to the 12-day orbital period of Imp 7 and the relatively slow variations in intensity in 6 hours. It is also apparent that the instrumental background is much lower than the intensities typical of this study.

Results

Characteristics

The large data set available for this study permits characterization of the periods of moderately enhanced low-energy proton fluxes from day 273, 1972, to day 2, 1974, a period near solar minimum. A complete model for these enhancements must be able to account for the intensities, spectra, and composition observed.

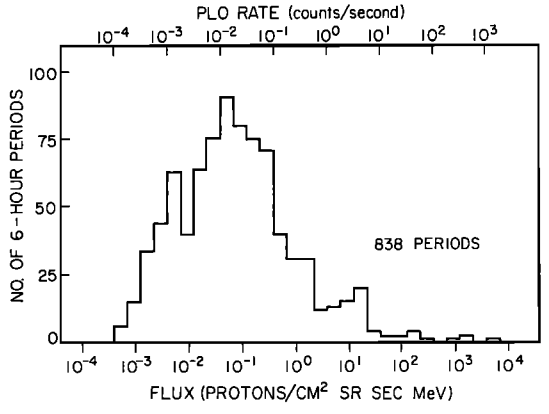

Fig. 4. The distribution of the flux of 1.2- to 2.4-MeV protons for data set 4*a*, excluding 13 periods when there were no counts.

Figure 4 shows the distribution of the intensity of 1.2- to 2.4-MeV protons for data set 2. Thirteen of the 851 6-hour periods in data set 2 have not been plotted because no particles were observed. The minimum nonzero intensity corresponds to one observed particle in a live time of ~3 hours (a flux of $\sim 4 \times 10^{-4}$ (cm² s sr MeV)$^{-1}$). Since only 1.6% of the periods have no counts, this minimum intensity does not substantially distort the distribution. The distribution resembles a log normal distribution with a high-flux tail due to prompt solar particle events. The sixteenth, fiftieth, and eighty-fourth percentiles of the nonzero intensities are at 0.005, 0.07 and 0.8 (cm² s sr MeV)$^{-1}$, respectively. Data set 4*b*, which lies between the fortieth and the ninetieth percentile, and data set 4*c* (sixtieth to ninetieth percentiles) are the basis for most of the subsequent analysis.

For each of the 6-hour periods used in this study, the energy spectrum has been characterized by a spectral index γ. The distribution of γ for data set 4*b* is shown in Figure 5. The mean and standard deviation of the distribution are 3.0 and 0.8, respectively. Values range from 1 to 5. As is indicated in Figure 5, the standard deviation of the distribution of γ is larger than the statistical uncertainty of the individual measurements and consequently is indicative of real variations in the spectrum.

These periods of moderately enhanced fluxes typically have softer spectra than the prompt solar particle events surveyed by *Van Hollebeke et al.* [1975]. The prompt events had a mean

spectral index of 2.4 for the energy interval 4–20 MeV when they were measured at the peak of the events. A softer spectrum was found for the energy interval 20–80 MeV. This suggests that there would be a harder spectrum from 1.3 to 2.3 MeV than from 4 to 20 MeV during prompt events, producing a difference larger than 0.6 in the average γ for the prompt events and the periods used in this study.

Previous studies of moderate increases have reported spectra which are generally consistent with the range of spectra shown in Figure 5. *Fan et al.* [1965] reported that the recurrent proton events in late 1964 had a γ of ~3.5, while the August 27, 1966, increase studied by *Fan et al.* [1968] had a γ of 2.5. *Roelof and Krimigis* [1973] found that γ was always greater than 1.5. Increases near 3 AU have been fit by *Van Hollebeke et al.* [1977] with exponential rigidity spectra of the form $dJ/dR \propto \exp(-R/R_0)$ with R_0 typically 8–15 MV. This corresponds to effective spectral indexes at 1.5 MeV of 2.3–3.8, a range of values similar to that in Figure 5. Thus the moderate increases included in the present extensive study appear to be spectrally similar to those included in earlier studies.

Composition

The composition of the particles in these periods of moderately enhanced flux reveals the source composition as modified by the acceleration and propagation of the particles. Figure 6 shows the distribution of the ratios of the flux of 1.4- to 2.4-MeV per nucleon alpha particles to the flux of 1.3- to 2.3-MeV protons for both flare and nonflare periods. The nonflare periods are data set 4*b*. The selection criteria for the flare periods are the same as those for the nonflare periods, except that the periods must occur on either the day of onset of one of the previously discussed 25 prompt solar particle events or the 2 days following an onset. Since the alpha particles typically have a softer spectrum than the protons, the ratio will be energy dependent. For typical spectra, adjusting the proton energy bins to correspond to the energy bin of the alpha particles would multiply the alpha-to-proton ratios in Figure 6 by 1.20 ± 0.06.

The ensemble average alpha-to-proton ratios of 2.5% for flare periods and 3.3% for nonflare periods are similar. These ratios are also similar to the typical alpha-to-proton ratio in the solar wind of ~4.5% as reviewed by *Bame* [1972]. The distributions of the alpha-to-proton ratios are, however, quite different. The distribution for flare periods is much broader than that for nonflare periods and is peaked at a lower alpha-to-proton ratio. The distribution of ratios in the solar wind is also broader than that for nonflare periods, with values ranging from 1% to more than 20%. An acceleration model using

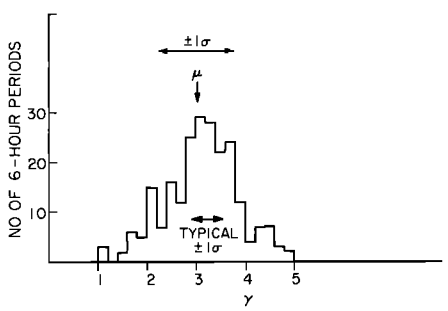

Fig. 5. The distribution of the spectral index γ for data set 4*b*. The mean μ and standard deviation σ of the distribution are indicated as well as the typical statistical uncertainty of an individual measurement.

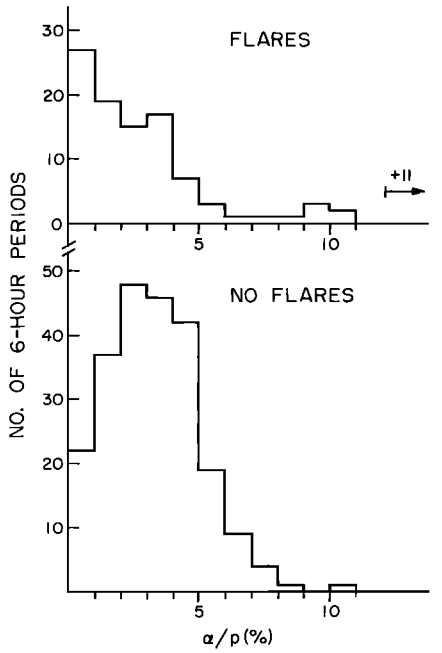

Fig. 6. The distribution of the ratio of 1.4- to 2.4-MeV per nucleon alpha particles to 1.3- to 2.3-MeV protons for both flare and nonflare periods. Data set 4*b* is used for the nonflare periods. The ratio should be multiplied by 1.20 ± 0.06 to obtain the ratio at 1.4–2.4 MeV per nucleon.

solar wind plasma as a source may therefore have to be consistent with a wider variation in the composition of the source particles than in the accelerated particles.

Figure 7 shows the alpha-to-proton ratio as a function of V. Little dependence is evident for $V < 600$ km/s, but the highest-speed streams have significantly higher alpha-to-proton ratios. This result, however, is based on only a few high-speed streams and so needs to be confirmed by further observations. At 2.7-MeV total energy, *Gold et al.* [1975] reported one recurrent α rich stream which was associated with a recurrent high-speed stream and one which was not.

McDonald et al. [1976] and *Barnes and Simpson* [1976] report that the increases observed near 3 AU are associated with high-speed streams in the solar wind. Such an association might also be expected at 1 AU. Figure 8 shows, as a function of V, both the mean and the median proton intensity for data

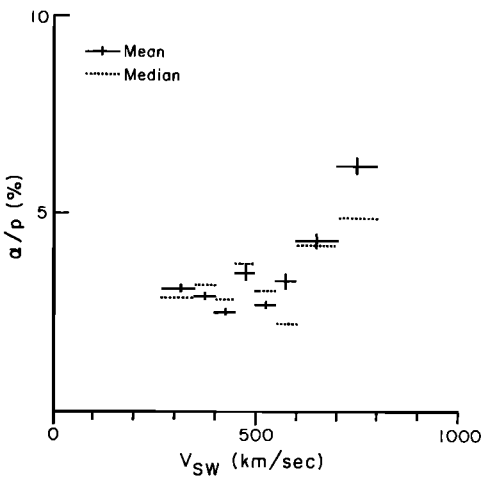

Fig. 7. The mean and median alpha-to-proton ratio as a function of solar wind velocity for data set 4*b*.

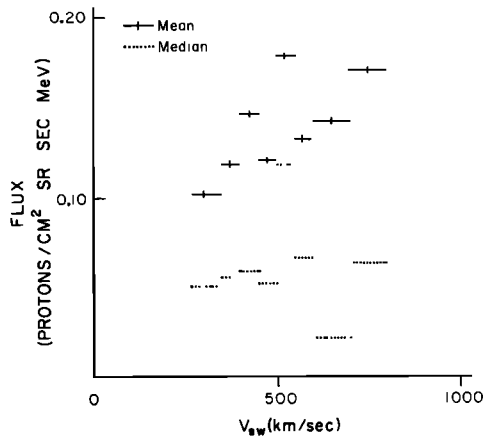

Fig. 8. The mean and median flux of 1.2- to 2.4-MeV protons as a function of solar wind velocity for data set 4*a*.

set 4*a*. No clear trend is seen in the medians, although the means are larger at higher V. This is the result of the skewing of the distribution of intensities toward larger intensities during periods of high V.

Proton Anisotropy

Figure 9*a* shows ξ_{obs} for the 122 6-hour periods comprising data set 4*c*. Somewhat more than half these periods (60%) have a decreasing intensity. The mean x and y components of the anisotropy are $\langle\xi_{obs}\rangle_{x,y} = (-7.4 \pm 1.1\%, -2.6 \pm 1.1\%)$. Weighted means are used, with each 6-hour value weighted according to the statistical uncertainty in the anisotropy measurement. Since the 6-hour points are more dispersed about the mean than is expected from purely statistical uncertainties, there are real variations in the anisotropy. As a result, the uncertainties quoted for this and subsequent mean anisotropies are based on the observed rms variation of the 6-hour values about the mean values.

For each of these 122 periods the measured spectral index γ and the solar wind speed V have been used in (1) to determine ξ_{dif}, which has been plotted in Figures 9*b* and 9*c*. Figure 9*b* uses the same SE coordinates as are used in Figure 9*a*. The mean x and y components of ξ_{dif} are $\langle\xi_{dif}\rangle_{x,y} = (14.0 \pm 1.2\%, -3.9 \pm 1.1\%)$. Thus although the mean observed streaming is from the sun, the mean diffusive streaming is toward the sun.

In Figure 9*c*, ξ_{dif} is replotted, but the coordinate system has been rotated about the z axis, so that the x axis, relabeled $x_{\parallel}$, is colinear with the average magnetic field direction for that 6-hour period. Positive $x_{\parallel}$ is defined to lie within 90° of 315° in SE coordinates. Nominally, flow back toward the sun along the field has a positive component along $x_{\parallel}$. However, when the field is nearly perpendicular to its long-term average direction, it is not obvious which direction leads toward the sun, and the wrong direction may have been chosen for approximately eight such periods. The mean components parallel to and perpendicular to the field are $\langle\xi_{dif}\rangle_{\parallel,\perp} = (11.9 \pm 1.5, 1.4 \pm 0.9)$.

As was indicated by (1), the diffusive anisotropy produced by a spatial gradient depends on κ, which is not known. In particular, the relative amounts of diffusion perpendicular to and parallel to the magnetic field are unresolved. Perpendicular diffusion has been regarded as negligible [*Wibberenz*, 1974] and as comparable to parallel diffusion [*Jokipii*, 1971]. To encompass this range of possible perpendicular diffusion, we determine the sign of the radial gradient both for negligible perpendicular diffusion and for isotropic diffusion. For isotropic diffusion the 87% of the periods in Figure 9*b* having a positive x component indicates that 87% of these periods have a positive radial gradient. Similarly, for diffusion only parallel to the magnetic field the data in Figure 9*c* indicate that 79% of the periods have a positive gradient along the field away from the sun. Thus for either case, ξ_{dif} indicates that U is typically larger outside 1 AU than it is inside 1 AU. This gradient is opposite that produced by continuous injection of MeV protons by the sun.

For particles with the same energy in the solar wind frame, *Jokipii and Parker* [1970] have shown that the anisotropy in the sun-fixed frame is $\xi_{part} = 3(\mathbf{V} - \kappa\nabla U/U)w$. In the anisotropic diffusion approximation the solar wind frame is unique in that there is no electric field and the particles elastically scatter from the scattering centers which are at rest with respect to the solar wind. In this frame the particles to first order in V/w do not change energy when they scatter; ξ_{part} differs from ξ_{obs} in that there is no Compton-Getting factor, consistent with the fact that the streaming of individual particles must be independent of the flux at other energies. A histogram of $\xi_{part,x}$ for data set 4*b* is shown in Figure 10. The average radial component of ξ_{part} is 5% ± 1% with flow toward the sun. This corresponds to an energy flow toward the sun of 1.3×10^{-7} erg $(cm^2\ s)^{-1}$ of 1.3- to 2.3-MeV protons. This energy flow is 4×10^{-7} of the energy in the bulk flow of the solar wind. The individual particles are diffusing toward the sun

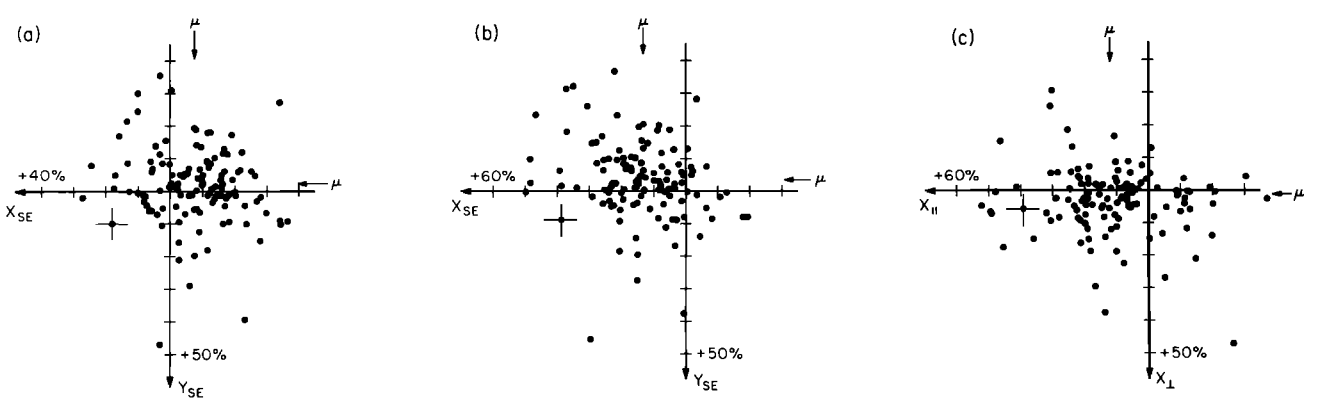

Fig. 9. (*a*) Six-hour averages of the observed anisotropy ξ_{obs} for data set 4*c*. A typical $\pm 1\sigma$ error bar is shown. The means μ of the x and y components are indicated by arrows. (*b*) Six-hour averages of the diffusive anisotropy ξ_{dif}. (*c*) Six-hour averages of the components of ξ_{dif} parallel to and perpendicular to the average magnetic field direction for the 6-hour period.

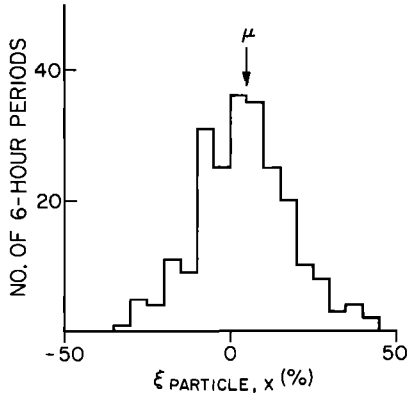

Fig. 10. The distribution of the x component of ξ_{part} for data set 4*b*. The mean value μ is indicated.

faster than they are being convected away from the sun, a sink of 1.3- to 2.3-MeV protons inside 1 AU being indicated.

To understand better the source of these particles and their propagation in the interplanetary medium, the dependence of the anisotropy on various parameters has been examined. Data set 4*a* has been used to show that the diffusive flow toward the sun reported above is typical for a wide range of intensities. Four groups of intensities, covering a dynamic range of 100, are shown in Figure 11. The distributions of anisotropies for the four groups are similar with means ranging from 10% to 15%. For intensities less than 0.012 (cm² s sr MeV)$^{-1}$, anisotropies computed for 6-hour periods have very large statistical errors. Consequently, the data for all these periods have been summed, and $\langle\xi_{dif,x}\rangle$ is 11% ± 4%. Thus the diffusive anisotropy is at least qualitatively independent of the intensity during these periods.

The diffusive anisotropy is also largely independent of the alpha-to-proton ratio. The best least squares linear fit to $\xi_{dif,x}$ as a function of α/p is $\xi_{dif,x} = (9.7\% \pm 0.9\%) + (130 \pm 24)\alpha/p$. However, χ_ν^2 is 6.2, indicating that there is more scatter to the data with respect to the fitted function than is expected from the measurement uncertainties. The correlation coefficient is 0.18; there is only a 2.5% probability that uncorrelated data would result in a positive correlation coefficient this large or larger. The observed degree of correlation is most likely the result of the already noted dependence of α/p on V together with the dependence of $\xi_{dif,x}$ on V discussed below.

The diffusive anisotropy ξ_{dif} should provide information on the diffusion tensor κ, especially with respect to diffusion parallel and perpendicular to the magnetic field. If $\kappa_\perp$ is much less than $\kappa_\parallel$, then ξ_{dif} will be nearly aligned with **B**. However, for isotropic diffusion ($\kappa_\perp = \kappa_\parallel$) the direction of ξ_{dif} will be independent of the direction of **B**.

Previous observations have yielded varied results. *McCracken et al.* [1968] found a strong dependence of the direction of ξ_{obs} on the direction of the magnetic field during the early parts of prompt solar particle events. This dependence was interpreted by the authors as being due to a field-aligned ξ_{dif}. In contrast, *Allum et al.* [1974] found that late in prompt solar particle events, the observed anisotropy direction was independent of the observed magnetic field direction. *Pesses and Sarris* [1975] have reported 15-min periods for which they conclude that ξ_{dif} could not be field aligned.

The present work differs from these previous studies in that ξ_{dif} rather than ξ_{obs} is used. A large part of ξ_{obs} is ξ_{con}, which is unrelated to the magnetic field. In Figure 12 the direction of the diffusive anisotropy ϕ_{dif} is plotted as a function of the

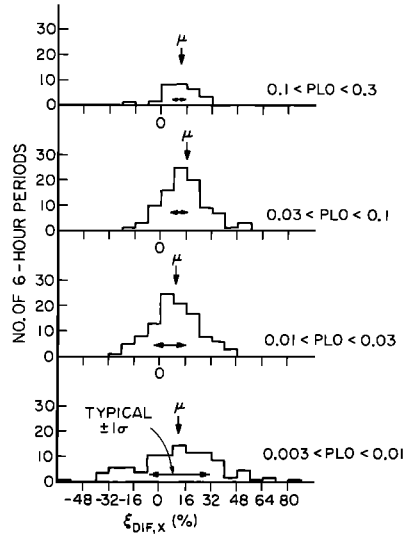

Fig. 11. The distribution of the x component of ξ_{dif} for four intervals of the proton intensity as monitored by the PLO rate. The 6-hour periods used are from data set 4. From highest intensity down, the mean values μ are (12.7 ± 0.7)%, (15.2 ± 0.6)%, (9.7 ± 1.0)%, and (10.8 ± 1.8)%. The ±1σ typical uncertainties for individual 6-hour periods are also shown.

magnetic field direction ϕ_B. The raw ϕ_{dif} data are shown in the left panel; ϕ_B has been restricted to a 180° range by using the observed field direction modulo 180°. The best linear fit to the data in the left panel is shown in the right panel. The fitting procedure has been designed to accommodate the fact that for every ϕ_B there are two field-aligned flow directions corresponding to flow toward and away from the sun. Hence in the right panel the adjusted values of ϕ_{dif} have been mapped to within 90° of the fit by adding an integral multiple of 180° to ϕ_{dif}. The fit with the minimum χ_ν^2 is $\phi_{dif} = -(8.5° \pm 1.3°) + (0.74 \pm 0.03)\phi_B$.

The fit shows the strong dependence of the diffusive flow on the direction of the magnetic field. In terms of the diffusion coefficients, $\kappa_\parallel > \kappa_\perp$. The data are not consistent with diffusion only along $\langle\mathbf{B}\rangle$, a finding suggesting that flow perpendicular to the average field is not negligible. Since 6-hour averages have been used for both the field direction and the anisotropy, there is a possibility that the averaging process has reduced the dependence of ϕ_{dif} on ϕ_B and that on a shorter time scale the flow is field aligned.

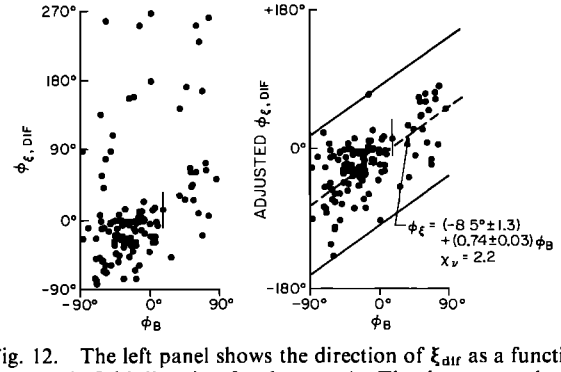

Fig. 12. The left panel shows the direction of ξ_{dif} as a function of the magnetic field direction for data set 4*c*. The data are replotted in the right panel such that points which would have been plotted outside the solid lines have had +180° or −180° added to their anisotropy direction. The dashed line, which determines the position of the solid lines, is the least squares fit to the data. A typical ±1σ error bar is indicated.

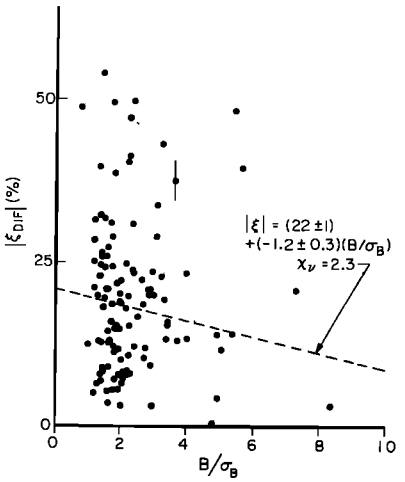

Fig. 13. The dependence of the amplitude of ξ_{dif} on the relative fluctuations in the magnetic field for data set 4c. A typical $\pm 1\sigma$ error bar is indicated. The dashed line is the least squares fit to the data.

Another interesting factor is that the χ_ν value of 2.2 in Figure 12 indicates that the dispersion of the direction of ξ_{dif} about the direction of the B field is about twice as large as is expected from statistical fluctuations alone. An understanding of this residual dispersion requires further study.

Equation (1) indicates that changes in κ would affect ξ_{dif} unless they are compensated by changes in the density gradient. *Jokipii* [1966] has related κ to fluctuations in the magnetic field with wavelengths comparable with the diffusing particle's Larmor radius. The present work has sufficient information only to estimate the fluctuations in the magnetic field over a wide range of frequencies, from $\sim 3 \times 10^{-4}$ s^{-1} to ~ 1 s^{-1}. Since the frequency appropriate for 1.5-MeV protons is $\sim 10^{-2}$ s^{-1}, variation in power in the above frequency interval should be an approximate indication of the relative amount of scattering of the observed protons. Thus a dimensionless parameter given by B/σ_B is used, where σ_B is the standard deviation in the fine time scale averages used to determine the hourly average magnetic field. A smaller κ is predicted for larger fluctuations (i.e., for smaller B/σ_B), which for constant gradients would produce a smaller ξ_{dif}. Figure 13 is a plot of ξ_{dif} as a function of the average of the hourly B/σ_B for the 6-hour period. The best linear fit to the data is also indicated. In view of the large χ_ν for the fit the difference of the slope from zero is not considered significant. This result is consistent with a diffusive anisotropy independent of the magnitude of the local κ. Such independence would result from the steady state propagation model discussed below.

If the periods of moderately enhanced fluxes of this study were related to prompt solar particle events, then the diffusive anisotropy might be dependent on the time elapsed since the most recently observed prompt event. In Figure 14, $\xi_{\parallel}$ for data set 4c is plotted as a function of the time since the onset of the most recently observed prompt event. The plot shows the wide range of times since the most recent event for the periods in the data set. There is considerable scatter in the plot but no apparent trend as a function of time. This lack of a trend is also indicated by the linear fit made to the data. Thus there is no evidence that these moderately enhanced periods are related to the prompt events.

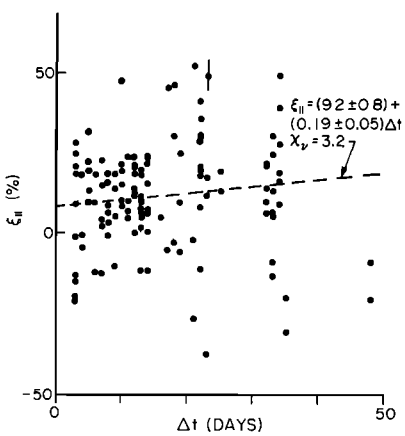

Fig. 14. The dependence of the component of the diffusive anisotropy parallel to the magnetic field on the number of days since the onset of the most recent identified prompt solar particle event. The data are from data set 4c.

Anisotropy Model

Earlier observations of these periods of moderately enhanced intensities have shown their recurrent character. This long-term coherence suggests that the propagation of these particles might reasonably be approximated by the steady state propagation equation

$$\nabla\cdot(\kappa\cdot\nabla U) - \nabla\cdot(U\mathbf{V}) + \tfrac{1}{3}\nabla\cdot\mathbf{V}\frac{\partial}{\partial T}[\alpha(T)TU] = 0 \quad (3)$$

Several simplifying assumptions have been made: (1) there is azimuthal symmetry, (2) the radial diffusion coefficient κ_{rr} is independent of energy and radius, (3) V is radial and independent of position, (4) U is finite at $r = 0$, and (5) there is a source of particles at some $r > 1$ AU. Similar assumptions were used by *Lupton and Stone* [1973] to fit time profiles of prompt solar particle events. The solution to (3) is of the form

$$U(r) = U_K(-2C + 2;\ 2;\ -Vr/\kappa_{rr})\exp(Vr/\kappa_{rr}) \quad (4)$$

in which U_K is a solution to Kummer's equation. U increases approximately exponentially away from $r = 0$ with a scale length of $\sim\kappa_{rr}/V$. *Fisk and Axford* [1969] first discussed this solution in a study of the modulation of galactic cosmic rays.

Equation (4) has been used to investigate the effect on the anisotropy of changes in κ_{rr} and V. As is shown in Figure 15, $\xi_{dif,x}$ is relatively independent of κ_{rr} for κ_{rr} between 10^{20} and 10^{22} cm^2/s. Changing κ_{rr} by a factor of 100 produces a change of less than a factor of 2 in $\xi_{dif,x}$. This very weak dependence in the model is consistent with the observed lack of dependence of ξ_{dif} on fluctuations in the magnetic field as discussed above.

On the other hand, $\xi_{dif,x}$ is approximately proportional to V. $\xi_{dif,x}$ is plotted as a function of V for two values of κ_{rr} in Figure 16. Also shown are the mean $\xi_{dif,x}$ for four velocity intervals of

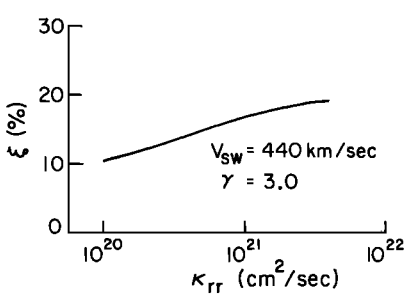

Fig. 15. The dependence of the x component of the diffusive anisotropy as a function of the radial diffusion coefficient κ_{rr} calculated by using the propagation model discussed in the text.

data set 4*b*. The observations are consistent with the model calculations for $\kappa_{rr} \sim 4 \times 10^{20}$ cm²/s.

This strong dependence on V and weak dependence on κ_{rr} can be viewed as competition between diffusion and convection. In a steady state the diffusive flow and the convective flow must approximately balance, except for losses. Thus if the effective convective velocity $w\xi_{con}/3$ increases because of an increase in V, the effective diffusive velocity $w\xi_{dif,x}/3$ will also increase. On the other hand, a change in κ_{rr} does not affect the effective convective velocity, and so the effective diffusive velocity is relatively insensitive to changes in κ_{rr}. The radial gradient, however, adjusts to compensate for the change in κ_{rr}.

This picture indicates that the radial gradient needed to produce the observed $\xi_{dif,x}$ depends on the value of κ_{rr}, which is not known. By using the mean observed γ of 3.0 and V of 477 km s^{-1} (obtained from data set 4*c* and weighted by the observed number of protons) the model produces diffusive anisotropies ranging from 10% to 16% for κ_{rr} from 10^{20} to 10^{21} cm²/s. An intensity ratio between 1 and 3 AU of 14, comparable with that suggested by Pioneer 11 data, is produced by a κ_{rr} of 10^{21} cm²/s. A ratio of 3 is produced between 0.3 and 1 AU. Larger gradients are produced by smaller values of κ_{rr}. These gradients between 1 and 3 AU will be smaller if particles are injected over a range of radii around 3 AU or if κ_{rr} increases with radius.

Alpha Particles

Anisotropies have also been determined for 1.4- to 2.4-MeV per nucleon alpha particles during these periods between prompt solar particle events. Because of the relatively small number of alphas the sectored counts and spectrum have been accumulated for all the 6-hour periods of data set 4*a*.

The spectral index for this integrated data set is 4.0 ± 0.5. The quoted uncertainty is due to systematic rather than statistical errors and is determined by using different methods to estimate the corrections that need to be made to the raw alpha spectrum. The mean solar wind velocity for the data set, weighted by the number of alphas observed, is 493 km/s. The average x and y components of the alpha anisotropy are $\langle\xi_{obs}\rangle$ = (−11% ± 2%, 0% ± 2%) and $\langle\xi_{dif}\rangle$ = (16% ± 3%, −2% ± 2%).

Thus the alphas and protons have approximately the same mean diffusive anisotropy during these periods between prompt solar particle events, as would result from the anisotropy model discussed above.

CONCLUSION

The diffusive streaming of low-energy protons has been found to be predominantly toward the sun during periods between prompt solar particle events. This flow toward the sun occurs for essentially all proton intensities and solar wind velocities. The average radial component of this anisotropy (14%) and its dependence on the solar wind velocity are consistent with the anisotropy calculated by using a steady state propagation model including adiabatic energy loss for $\kappa_{rr} \sim 4 \times 10^{20}$ cm²/s. More sophisticated models will be needed to account for the detailed time variations.

The average radial component (16%) of the diffusive flow of low-energy alpha particles is very similar to that found for protons, a condition suggesting that the steady state propagation model for protons discussed above is also applicable to alphas.

Previous observations at 1 AU during periods between prompt events have been interpreted as indicating the sun to be a continuous source of MeV protons. These new observations show that such a direct solar source of either protons or alphas is rare during 1973.

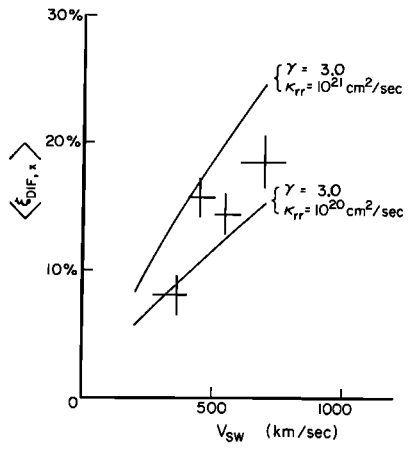

Fig. 16. The mean radial component of ξ_{dif} as a function of solar wind velocity for data set 4*c*. Anisotropies calculated by using the propagation model discussed in the text are shown by the solid curves.

At present it is not possible to identify the acceleration mechanism for these particles. However, many of the characteristics of the flux at 1 AU are relevant to the ultimate identification of this acceleration process. For example, the energy flow in 1.3- to 2.3-MeV particles is 1.3×10^{-7} erg cm^{-2} s^{-1} as measured by using data set 4*c*. Since this flow is only 4×10^{-7} of energy in the bulk flow of the solar wind, interplanetary acceleration is a possible source mechanism. The median flux for periods including prompt solar events is 0.07 (cm² s sr MeV)$^{-1}$ with 68% of the periods having fluxes between 0.005 and 0.8 (cm² s sr MeV)$^{-1}$. This study includes all intensities but those above the ninetieth percentile.

The proton spectrum during the periods between prompt solar events could be well fit by a power law. The distribution of spectral indices has a mean of 3.0 and a standard deviation of 0.8. This mean spectrum is softer than that reported as the mean at the peak intensity of prompt solar particle events.

The composition of the enhanced fluxes has been compared both with the composition of particles accelerated by solar flares and with the composition of solar wind plasma which might be a source of particles for interplanetary acceleration. The distributions of alpha-to-proton ratios have similar means, but the distribution for periods between prompt events is significantly narrower than that for prompt events or solar wind plasma. This suggests that the particles seen between prompt events are not accelerated in solar flares. If the particles are accelerated out of the solar wind, either the solar wind composition during these measurements was less variable than was reported from earlier studies or the acceleration process must result in less variability in the alpha-to-proton ratio than in the solar wind.

The flow of particles during these periods of moderately enhanced fluxes has also been used to study the propagation of energetic particles in the interplanetary medium. The dependence of the direction of the diffusive anisotropy has been directly compared with the direction of the magnetic field during periods of small anisotropy when the diffusive theory is valid. The direction of the diffusive anisotropy is strongly dependent on the field direction, a situation indicating $\kappa_\perp < \kappa_\parallel$. The two directions are not colinear, however. The data are thus consistent with nonnegligible flow perpendicular to the average field direction when averaged over a 6-hour interval.

Acknowledgments. We are grateful to H. S. Bridge and J. D. Sullivan for providing Imp 7 plasma data prior to publication. We are also grateful to R. E. Vogt, who has been intimately involved throughout the Imp 7 program. Significant contributions to this project have also been made by W. E. Althouse, G. J. Hurford, and R. A. Mewaldt. This work was supported in part by the National Aeronautics and Space Administration under contract NAS5-11066 and grant NGR 05-002-160. F. E. Marshall has received valuable support from an NDEA fellowship.

REFERENCES

Allum, F. R., R. A. R. Palmeira, K. G. McCracken, and U. R. Rao, Cosmic ray anisotropies observed late in the decay phase of solar flare events, *Solar Phys., 38,* 227, 1974.

Anderson, K. A., Electrons and protons in long-lived streams of energetic solar particles, *Solar Phys., 6,* 111, 1969.

Bame, S. J., Spacecraft observations of solar wind composition, Solar Wind, *NASA Spec. Publ., SP-308,* 170, 1972.

Barnes, C. W., and J. A. Simpson, Evidence for interplanetary acceleration of nucleons in corotating interaction regions, *Astrophys. J., 210,* L91, 1976.

Bryant, D. A., T. L. Cline, U. D. Desai, and F. B. McDonald, Continual acceleration of solar protons in the MeV range, *Phys. Rev. Lett., 14,* 481, 1965.

Fan, C. Y., G. Gloeckler, and J. A. Simpson, Protons and helium nuclei within interplanetary magnetic regions which co-rotate with the sun, *Proc. Int. Conf. Cosmic Rays, 1,* 109, 1965.

Fan, C. Y., M. Pick, R. Pyle, J. A. Simpson, and D. R. Smith, Protons associated with centers of solar activity and their propagation in interplanetary magnetic field regions corotating with the sun, *J. Geophys. Res., 73,* 1555, 1968.

Fisk, L. A., and W. I. Axford, Solar modulation of galactic cosmic rays, 1, *J. Geophys. Res., 74,* 4973, 1969.

Gold, R. E., S. M. Krimigis, E. C. Roelof, A. S. Krieger, and J. T. Nolte, Relation of large-scale coronal X-ray structure and cosmic rays, 3, Low-intensity solar particle events with enhanced ~3 MeV helium and medium fluxes associated with solar wind streams, *Proc. Int. Conf. Cosmic Rays 14th, 5,* 1710, 1975.

Hurford, G. J., R. A. Mewaldt, E. C. Stone, and R. E. Vogt, The energy spectrum of 0.16 to 2 MeV electrons during solar quiet times, *Astrophys. J., 192,* 541, 1974.

Jokipii, J. R., Cosmic-ray propagation, 1, Charged particles in a random magnetic field, *Astrophys. J., 146,* 480, 1966.

Jokipii, J. R., Propagation of cosmic rays in the solar wind, *Rev. Geophys. Space Phys., 9,* 27, 1971.

Jokipii, J. R., and E. N. Parker, On the convection, diffusion and adiabatic deceleration of cosmic rays in the solar wind, *Astrophys. J., 160,* 735, 1970.

Kinsey, J. H., Identification of a highly variable component in low-energy cosmic rays at 1 AU, *Phys. Rev. Lett., 24,* 246, 1970.

Krimigis, S. M., E. C. Roelof, T. P. Armstrong, and J. A. Van Allen, Low-energy (>0.3 MeV) solar particle observations at widely separated points (>0.1 AU) during 1967, *J. Geophys. Res., 76,* 5921, 1971.

Lupton, J. E., and E. C. Stone, Solar flare particle propagation: Comparison of a new analytic solution with spacecraft measurements, *J. Geophys. Res., 78,* 1007, 1973.

Marshall, F. E., The streaming of 1.3–2.3 MeV cosmic-ray protons during periods between prompt solar events, Ph.D. thesis, Calif. Inst. of Technol., Pasadena, 1977.

Marshall, F. E., and E. C. Stone, Persistent sunward flow of ~1.6 MeV protons at 1 AU, *Geophys. Res. Lett., 4,* 57, 1977.

McCracken, K. G., and U. R. Rao, Solar cosmic ray phenomena, *Space Sci. Rev., 11,* 155, 1970.

McCracken, K. G., U. R. Rao, and N. F. Ness, Interrelationship of cosmic ray anisotropies and the interplanetary magnetic field, *J. Geophys. Res., 73,* 4159, 1968.

McDonald, F. B., and U. D. Desai, Recurrent solar cosmic ray events and solar *M* regions, *J. Geophys. Res., 76,* 808, 1971.

McDonald, F. B., B. J. Teegarden, J. H. Trainor, and T. T. von Rosenvinge, The interplanetary acceleration of energetic nucleons, *Astrophys. J., 203,* L149, 1976.

Pesses, M. E., and E. T. Sarris, On the anisotropies of interplanetary low-energy proton intensities, *Geophys. Res. Lett., 2,* 349, 1975.

Roelof, E. C., and S. M. Krimigis, Analysis and synthesis of coronal and interplanetary energetic particle, plasma, and magnetic field observations over three solar rotations, *J. Geophys. Res., 78,* 5375, 1973.

Van Hollebeke, M. A. I., L. S. MaSung, F. B. McDonald, The variation of solar proton energy spectra and size distribution with helio longitude, *Solar Phys., 41,* 189, 1975.

Van Hollebeke, M. A. I., F. B. McDonald, J. H. Trainor, and T. T. von Rosenvinge, The radial variation of corotating particle streams in the inner and outer solar system, submitted to *Astrophys. J.,* 1977.

Wibberenz, G., Interplanetary magnetic fields and the propagation of cosmic rays, *J. Geophys., 40,* 667, 1974.

(Received July 18, 1977;
revised January 19, 1978;
accepted February 8, 1978.)